Intracavity Raman conversion of a red semiconductor disk laser using diamond

Peter J. Schlosser,[1,2] Daniele C. Parrotta,[1,*] Vasili G. Savitski,[1] Alan J. Kemp,[1] and Jennifer E. Hastie[1]

[1] *Institute of Photonics, Dept. of Physics, University of Strathclyde, 106 Rottenrow, Glasgow, G4 0NW, UK*
[2] *Currently with the Fraunhofer Centre for Applied Photonics, 347 Cathedral Street, Glasgow, G1 2TB, UK*
[*] *daniele.parrotta@strath.ac.uk*

Abstract: We demonstrate a diamond Raman laser intracavity-pumped by a red semiconductor disk laser (~675 nm) for laser emission at around 740 nm. Output power up to 82 mW of the Stokes-shifted field was achieved, limited by the available pump power, with an output coupling of 1.5%. We also report wavelength tuning of the diamond Raman laser over 736 - 750 nm.

OCIS codes: (140.3550) Lasers, Raman; (140.3600) Lasers, tunable; (140.5960) Semiconductor lasers; (140.7270) Vertical emitting lasers.

References and links

1. S. Calvez, J. E. Hastie, M. Guina, O. Okhotnikov, and M. D. Dawson, "Semiconductor disk lasers for the generation of visible and ultraviolet radiation," Laser & Photon. Rev. **3**, 407-434 (2009).
2. M. Fill, A. Khiar, M. Rahim, F. Felder, and H. Zogg, "PbSe quantum well mid-infrared vertical external cavity surface emitting laser on Si-substrates," J. of Appl. Phys. **109**, 093101 (2011).
3. J. A. Parish, "New concepts in therapeutic photomedicine: photochemistry, optical targeting and the therapeutic window," J. Investig. Dermat. **77**(1), 45-50 (1981).
4. B. Chance, M. Cope, E. Gratton, N. Ramanujam, and B. Tromberg "Phase measurement of light absorption and scatter in human tissue," Rev. Sci. Instr. **69**(10), 3457-3481 (1998).
5. J. E. Hastie, S. Calvez, M. D. Dawson, T. Leinonen, A. Laakso, J. Lyytikäinen, and M. Pessa, "High power CW red VECSEL with linearly polarized TEM_{00} output beam," Opt. Express **77**(13), 77-81 (2004).
6. D. P. Bour, R. S. Geels, D. W. Treat, T. L. Paoli, F. Ponce, R. L. Thornton, B. S. Krusor, R. D. Bringans, and D. F. Welch, "Strained $Ga_xIn_{(1-x)}P/(AlGa)_{0.5}In_{0.5}P$ heterostructures and quantum-well laser diodes," IEEE J. Quantum Electron. **30**(2), 593-607 (1994).
7. P. J. Schlosser, J. E. Hastie, S. Calvez, A. B. Krysa, and M. D. Dawson, "InP/AlGaInP quantum dot semiconductor disk lasers for CW TEM_{00} emission at 716-755 nm," Opt. Express **17**(24), 21782–21787 (2009).
8. A. Rantamäki, J. Rautiainen, J. Lyytikäinen, A. Sirbu, A. Mereuta, E. Kapon, and O. G. Okhotnikov, "1 W at 785 nm from a frequency-doubled wafer fused semiconductor disk laser," Opt. Express **20**(8), 9046-9051 (2012).
9. H. M. Pask, "Continuous-wave, all-solid-state, intracavity Raman laser" Opt. Lett. **30**(18), 2454–2456 (2005).
10. D. C. Parrotta, W. Lubeigt, A. J. Kemp, D. Burns, M. D. Dawson, and J. E. Hastie, "Continuous-wave Raman laser pumped within a semiconductor disk laser cavity," Opt. Lett. **36**(7), 1083-1085 (2011).
11. D. C. Parrotta, A. J. Kemp, M. D. Dawson, and J. E. Hastie, "Tunable continuous-wave diamond Raman laser," Opt. Express **19**(24), 24165-24170 (2011).
12. J. Lin, H. M. Pask, D. J. Spence, C. J. Hamilton, and G. P. A. Malcolm, "Continuous-wave VECSEL Raman laser with tunable lime-yellow-orange emission," Opt. Express **20**(5), 5219-5224(2012).
13. D. C. Parrotta, A. J. Kemp, M. D. Dawson, and J. E. Hastie, "Multi-Watt, continuous-wave, tunable diamond Raman laser with intracavity frequency doubling to the visible region," IEEE J. Sel. Top. Quantum Electron. **19**(4), 1400108 (2013).
14. A. A. Kaminskii, V. G. Ralchenko, and V. I. Konov, "CVD-diamond, a novel $\chi^{(3)}$-nonlinear active crystalline material for SRS generation in very wide spectral range," Laser Phys. Lett. **3**(4), 171-177 (2006).
15. I. Friel, S. L. Geoghegan, D. J. Twitchen, and G. A. Scarsbrook, "Development of high quality single crystal diamond for novel laser applications," Proc. of the SPIE **7838**, 783819 (2010).
16. V. G. Savitski, I. Friel, J. E. Hastie, M. D. Dawson, D. Burns, and A. J. Kemp, "Characterization of single-crystal synthetic diamond for multi-Watt continuous-wave Raman lasers," IEEE J. Quantum Electron. **48**(3), 328-337 (2012).

17. V. G. Savitski, S. Reilly, and A. J. Kemp, "Steady-state Raman gain in diamond as a function of pump wavelength," IEEE J. Quantum Electron. **49**(2), 218-223 (2013).
18. R. P. Mildren, J. E. Butler, and J. R. Rabeau, "CVD-diamond external cavity Raman laser at 573 nm," Opt. Express **16**(23), 18950–18955(2008).
19. A. Sabella, J. A. Piper, and R. P. Mildren, "1240 nm diamond Raman laser operating near the quantum limit," Opt. Lett. **35**(23), 3874-3876 (2010).
20. W. Lubeigt, V. Savitski, G. M. Bonner, S. L. Geoghegan, I. Friel, J. E. Hastie, M. D. Dawson, D. Burns, and A. J. Kemp, "1.6 W continuous-wave Raman laser using low-loss synthetic diamond," Opt. Express **19**(7), 6938-6944 (2011).
21. O. Kitzler, A. McKay, and R. P. Mildren, "Continuous-wave wavelength conversion for high-power applications using an external cavity diamond Raman laser", Opt. Lett. **37**(14), 2790-2792 (2012).
22. E. Granados, D. J. Spence, and R. P. Mildren, "Deep ultraviolet diamond Raman laser," Opt. Express **19**(11), 10857-10863 (2011).
23. A. Sabella, J. A. Piper, and R. P. Mildren, "Diamond Raman laser with continuously-tunable output from 3.38 to 3.80 μm," Opt. Lett. **39**(13), 4037-4040 (2014).
24. J. Caird, S. Payne, P. Staber, A. Ramponi, L. Chase, and W. Krupke, "Quantum electronic properties of the $Na_3Ga_2Li_3F_{12}:Cr^{3+}$ laser," IEEE J. Quantum Electron. **24**(6), 1077-1099 (1988).
25. D. J. Spence, "Spatial and spectral effects in continuous-wave intracavity Raman lasers," IEEE J. Sel. Top. Quantum Electron. **21**(1), 1400108 (2014).
26. R. P. Mildren (ed.) and J. R. Rabeau (ed.), *Optical Engineering of Diamond* (Wiley-VCH, 2013), Chap. 1.
27. A. K. McQuillan, W. R. L. Clements, and B. P. Stoicheff, "Stimulated Raman emission in diamond: spectrum gain and angular dispersion of intensity," Phys. Rev. A **1**(3), 628-635 (1970).
28. M. Grimsditch, M. Cardona, J. M. Calleja, and F. Meseguer, "Resonance in the Raman scattering of CaF_2, SrF_2, BaF_2 and diamond," J. Raman Spectrosc. **10**(1), 77-81 (1981).
29. M. S. Liu, L. A. Bursill, S. Prawer, and R. Beserman, "Temperature dependence of the first-order Raman phonon line of diamond," Phys. Rev. B **61**(5), 3391-3395 (2000).
30. G. M. Bonner, J. Lin, A. J. Kemp, J. Wang, H. Zhang, D. J. Spence, and H. M. Pask, "Spectral broadening in continuous-wave intracavity Raman lasers," **22**(7), 7492-7502 (2014).

1. Introduction

Semiconductor disk lasers (SDLs), also known as vertical-external-cavity surface-emitting lasers (VECSELs), have emerged as a commercial laser technology with great potential in terms of spectral coverage and power scalability. Direct emission of SDLs ranges from ~650 nm [1] to ~5 μm [2], while shorter wavelengths have been reached via nonlinear frequency upconversion [1]. Though bandgap engineering provides exceptional wavelength flexibility, there are certain spectral regions that cannot easily be reached by SDLs. One of these 'difficult' spectral regions is the 700-800 nm range, which coincides with the so-called 'therapeutic [optical] window', interesting for applications such as photomedicine [3-4]. Red-emitting SDLs utilize strained GaInP/AlGaInP quantum well (QW) heterostructures [1, 5], providing TE-polarized optical gain from ~640-700 nm [6]; however, we demonstrated that longer wavelengths can be achieved (716-755 nm shown) via the insertion of InP quantum dots (QDs) within the GaInP QW layers, to form a dot-in-a-well (DWELL) structure [7]. The output power of those lasers was limited to a few tens of mW due to non-optimised thermal offset of gain and resonances in the complex gain structure. More recently the longer wavelengths of this spectral region have been reached via frequency up-conversion; Rantamäki et al. demonstrated a frequency–doubled wafer-fused AlGaInAs QW SDL emitting up to 1 W at 785 nm [8].

Here we propose a different method to achieve laser operation in the 700-800 nm spectral region, which is based on intracavity Raman conversion of a QW-based red-emitting SDL operating at ~675 nm. Intracavity-pumped Raman lasers are a convenient means to shift the emission wavelength of continuous wave lasers [9], and with a fixed Stokes shift and no phase-matching requirements they can track the broad tuning range of the SDLs. We have previously demonstrated Raman conversion of tunable infrared SDLs based on InGaAs [10-11] and subsequently cascaded nonlinear conversion to the yellow-orange spectral range was achieved [12-13].

Among the several crystalline Raman media available, synthetic single-crystal diamond grown via chemical vapour deposition (CVD) is one of the most promising as it has good optical quality (birefringence $\Delta n \sim 10^{-6}$, absorption coefficient <1% cm^{-1}), very large Stokes shift (1332 cm^{-1}), high Raman gain coefficient (values up to ~20 cm/GW at 1 μm reported), unrivalled thermal conductivity (~2000 W m^{-1} K^{-1}), and broad optical transparency (from 225 nm to 2.5 μm and >6.5 μm) [14-17]. Diamond Raman lasers have been developed both in pulsed [18-19] and continuous-wave [13, 16, 20, 21] operation, and have been used for the generation of ultraviolet [22], visible [18], near infrared [11, 13, 16, 20, 21] and mid infrared light [23].

2. SDL design and characterization

The semiconductor disk laser (SDL) structure used in this work consisted of an $(Al_{0.6}Ga_{0.4})_{0.51}In_{0.49}P$ based active region, incorporating 20 compressively-strained, 6-nm-thick $Ga_{0.46}In_{0.54}P$ QWs, which were grouped in pairs at the ten available standing wave field antinodes for resonant periodic gain (RPG). The pump absorbing barrier material was lattice-matched to the GaAs substrate. The gain region was grown on top of a highly reflective (HR) distributed Bragg reflector (DBR), having 40.5 pairs of $Al_{0.45}Ga_{0.55}As$/AlAs with the reflectance stopband centre wavelength at 680 nm. The subcavity was set to be resonant at the design emission wavelength of 675 nm with a 15 nm offset between the QW photoluminescence peak at room temperature and the RPG wavelength. A commercial frequency-doubled YVO_4 solid-state laser emitting at 532 nm was used to pump the SDL, with a focus diameter $\varnothing_{pump}$ = 75 μm. For thermal management, an uncoated, 500-μm-thick CVD-grown single crystal diamond was optically contacted to the intra-cavity surface of the SDL and the bonded structure was clamped into a water-cooled brass mount with the circulating water kept at ~7 °C.

The SDL gain structure was incorporated in a 4-mirror cavity, with the DBR of the SDL structure as one plane end mirror, a HR folding mirror of 100 mm radius of curvature, a plane folding mirror and a plane end mirror. A maximum output power of P_{max} = 0.8 W (OC = 7.2%) was achieved for 4.1 W absorbed pump power, with a slope efficiency of $\eta_{diff} \approx 28\%$ with respect to the absorbed pump power. The internal loss of the SDL was estimated via Caird analysis to be L_{SDL} = 0.6% [24]. Wavelength tuning across a ~20 nm range (669.4 – 688.7 nm) was achieved using an intra-cavity 2-mm-thick quartz birefringent filter (see Fig. 1).

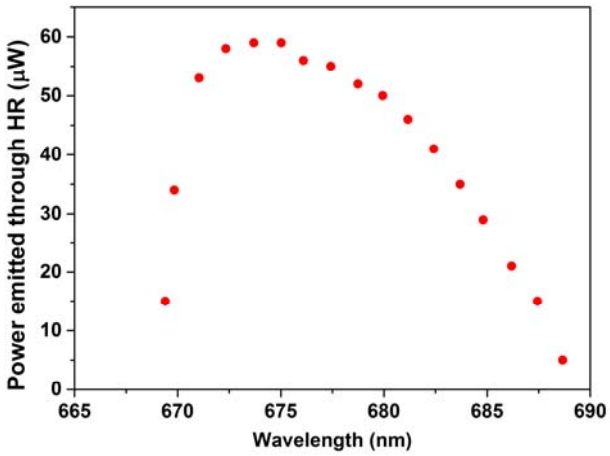

Fig. 1. Tuning curve of the red-emitting SDL in a high-finesse cavity (mirror transmission: 0.0007% at 675 nm) with a 2-mm-thick quartz birefringent filter.

3. CVD diamond characterization

The aforementioned diamond heatspreader and the diamond crystal now to be described for nonlinear frequency conversion were custom fabricated by Element Six Ltd. The dimensions of the CVD diamond used as the Raman medium were 2 x 2 x 8 mm^3. The crystal was specified to have low absorption and low birefringence. Measurements of the birefringence (Δn) provided by the manufacturer (using the Metripol technique) varied from $2.2 - 2.7 \cdot 10^{-6}$ in the direction of propagation.

In order to reduce intracavity losses, an anti-reflective (AR) coating was applied to both 2 x 2 mm^2 facets, allowing the 8 mm length of the crystal to be utilized for efficient Raman conversion. The centre wavelength of the AR coating was 710 nm with a specified (by the coating manufacturer) reflectance coefficient of $R_{AR} < 0.1\%$ from 670 to 750 nm. The diamond Raman crystal was cut for beam propagation along a <110> direction and oriented so that the horizontal polarization of the SDL was parallel to a <111> direction to have access to the largest Raman gain coefficient [16, 19]. For this crystal orientation the Raman gain coefficient in diamond has been estimated to be ~41 cm/GW at a pump wavelength of 670 nm [17].

We estimated the loss associated with the insertion of the diamond in the SDL cavity using Caird analysis. The total round trip loss in the SDL cavity was calculated to be 2.0 ± 0.4%, of which, from the previous Caird analysis, 0.6% was due to the SDL, leading to estimated diamond round trip losses of 1.4 ± 0.4%. The reflectivity of the AR coating was ~0.05% at 675 nm (from the theoretical curve provided by the coating manufacturer), so the round-trip loss due to the AR coating is ~0.2%. The remaining round trip loss (~1.2 ± 0.4%) was therefore assumed to be mostly due to absorption induced by the presence of nitrogen impurities. The corresponding absorption coefficient is estimated to be $<0.0075 \pm 0.0025$ cm^{-1} at 675 nm, which is comparable with the absorption loss measured for other diamond Raman crystals [16, 20, 21].

4. Experimental realization and results

The experimental configuration is illustrated in Fig. 2. The pump beam is focused onto the SDL chip to a $Ø_p = 75$ µm spot size by a 300 mm focal length plano-convex lens. The SDL-diamond heatspreader composite was clamped into a water-cooled brass mount (water temperature 7 °C) for thermal management. All mirrors of the fundamental cavity were HR for both fundamental and Stokes shifted fields. The folding mirrors (FM) had radii of curvature of 100 mm (FM1) and 50 mm (FM2), while the end mirror (M3) had radius of curvature of 50 mm. The cavity for the fundamental 675 nm field consisted of three cavity arms: SDL-FM1 = 61 mm, FM1-FM2 = 400 mm and FM2-M3 = 82.5 mm. A 4-mm-thick BRF was inserted at Brewster's angle within the SDL cavity, but outside the Raman

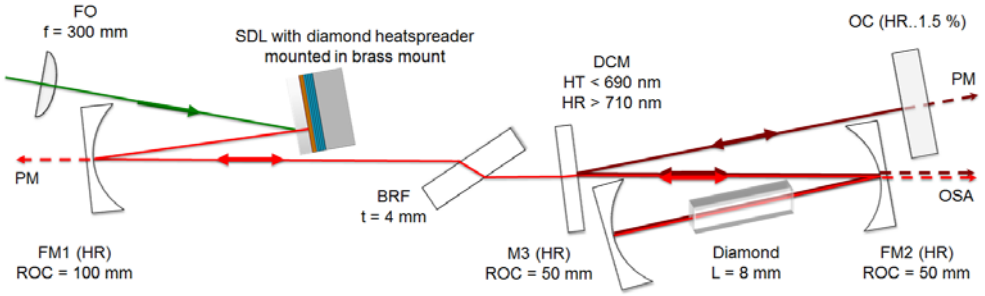

Fig. 2. Schematic of the cavity configuration. FO - Pump focusing optics, FM - folding mirror, M3 – end mirror for both the VECSEL and the Raman laser, HR – high reflector, ROC – radius of curvature, BRF - birefringent filter, DCM - dichroic mirror, OC - output coupler for the Stokes shifted field, PM - power meter, OSA - optical spectrum analyser.

resonator, for wavelength tuning and spectral narrowing of the SDL field. A narrow fundamental spectrum is important for efficient Raman conversion, as the presence of multiple peaks reduces conversion efficiency for each of the fundamental modes, due to competition for the available fundamental pump field [13]. FM2-M3 contained the 8-mm-long diamond crystal, positioned at the beam waist, calculated to be $Ø_D \approx 39$ µm in both the sagittal and tangential directions, and oriented for Raman excitation along <111>. This nearly round beam waist was achieved with small folding angles (<10°) at both folding mirrors, FM1 and FM2. The Stokes shifted field was separated from the fundamental by a dichroic mirror (DCM) with HR > 710 nm and high transmission, HT < 690 nm, placed inside the cavity with a small tilt of 7°. The coupled cavity for the Stokes shifted field was completed by a plane output coupler (OC) mirror with transmission of 1.5% from 690-795 nm. The combined distances between FM2-DCM and DCM-OC was 190 mm in order to match the beam waist size of the Stokes shifted field to that of the fundamental field inside the diamond crystal. The leakage through FM1 was used to monitor the intracavity power of the fundamental field. The optical spectra of both the fundamental and the Stokes shifted fields were monitored through FM2 using a fibre-coupled optical spectrum analyser (Anritsu MS9710C).

Figure 3 illustrates the power transfer curve for the maximum available output coupling of the Stokes field (1.5% OC). The laser threshold of the fundamental field was at ~0.7 W of absorbed pump power. Raman conversion was observed when the absorbed pump power was greater than 2.8 W and the intracavity power of the SDL was at least 10 W. Above threshold, the Raman laser output power increased linearly (slope efficiency ~7%) up to 82 mW, limited by the maximum available absorbed pump power (4 W). The spectra in the inset of Fig. 3 show that both the SDL and the Raman laser emitted within a single etalon peak (etalon due to the plane heatspreader in the SDL cavity) with emission linewidth ≤0.05 nm (~1 cm^{-1}). Note that the spectral resolution of the optical spectrum analyser is 0.05 nm, thus this measurement

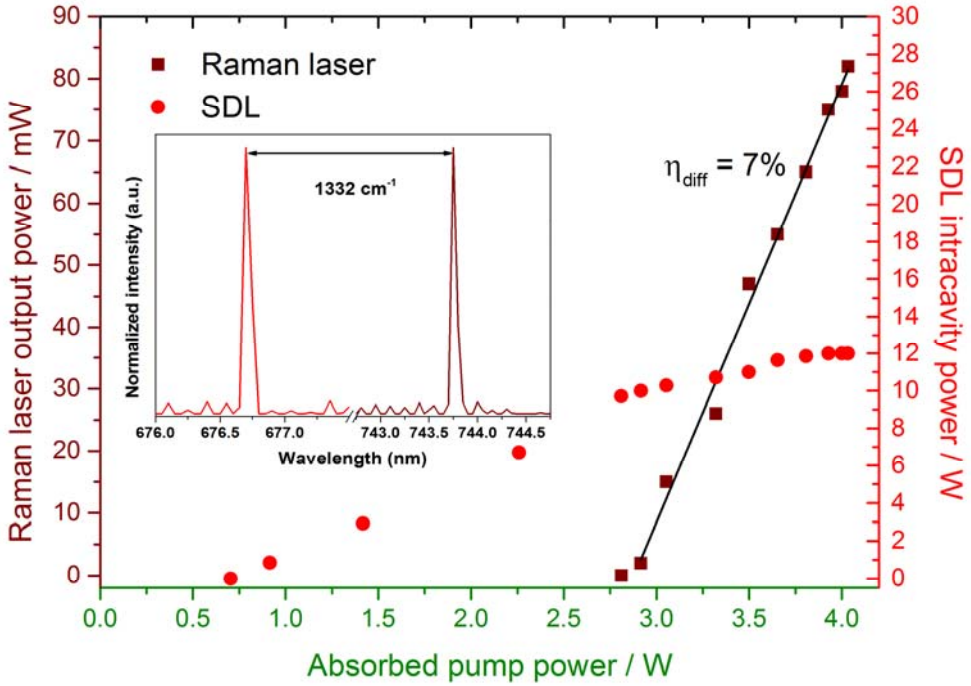

Fig. 3. Power transfer measurement of the Raman laser output power (dark red squares) through an OC = 1.5%, together with the monitored fundamental intracavity field (red circles). The inset shows the emission spectra of the SDL (red, left) and the Raman laser (dark red, right) at the maximum power.

is instrument-limited and the actual linewidths are likely to be narrower. While the fundamental emission did not show substantial spectral broadening as in our previous works [13], the SDL intracavity power did not clamp at its value at the Raman threshold (10 W), but gradually increased with the pump power up to 12 W. This rise of the fundamental intracavity power above the Raman threshold has been observed in other experiments and can be explained by suboptimal and power-varying spatial and spectral overlaps between the fundamental and the Stokes fields along the Raman crystal [13, 25].

For Raman laser emission of ~65 mW we measured the beam propagation factors (M^2) to be ~1.8 for the SDL and ~1.55 for the Raman laser. The polarization of the SDL was measured to be horizontal, which is to be expected when there is an intracavity birefringent filter inserted at Brewster's angle, while the polarization of the Raman laser was found to be ~13 degrees off horizontal. Rotation of the diamond crystal (±10° from the initial position) did not change the polarization of the Raman laser, thus we believe that the observed polarization mismatch was due to birefringence of the diamond sample rather than a misorientation of the Raman crystal as in [10].

Tuning of the fundamental field was possible via rotation of the BRF inside the fundamental cavity. For an absorbed pump power of 3.7 W the SDL emission was tunable over 12.5 nm (between 670.4-682.9 nm), limited by the free spectral range of the 4-mm-thick BRF. Figure 4 shows the simultaneous tuning of the fundamental and the Raman lasers (OC_{Stokes} = 1.5%) when the Raman field was allowed to oscillate. Almost the entire tuning range of the red SDL was Stokes shifted (670.8-682 nm), resulting in wavelength tuning of the Raman laser over 13.8 nm (from 736.6 to 750.4 nm), with maximum output power of 70 mW at 741.5 nm. This peak wavelength corresponds to the peak of the SDL tuning curve as shown in Fig. 1; however, Fig. 4 shows that the fundamental power emitted through the HR of the SDL during Raman oscillation, on the order of tens of μW, was higher at shorter wavelengths. This discrepancy between the tuning curves can be explained by noting that the transmission of the cavity optics (mirrors, Raman medium) are wavelength dependent, thus the shape of the tuning curve is set by the interplay between the SDL gain bandwidth, loss due to Raman conversion, and small changes in the spectral response of the optical elements within the two cavities.

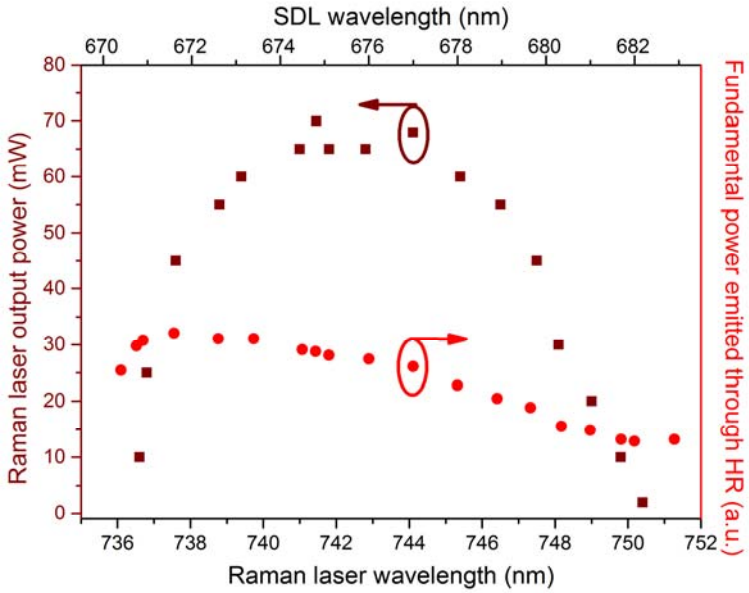

Fig. 4. Tuning of the fundamental (red circles) and the Stokes (dark red squares) fields for an absorbed pump power of 3.7 W, OC = 1.5 % and BRF thickness of 4 mm.

5. Data analysis

The results of these characterization measurements can be used to estimate the effective Raman gain of this laser and compare it with previous estimations of the Raman gain coefficient of diamond. In contrast to the Raman gain coefficient, the *effective* Raman gain depends on the spatial and spectral properties of the laser system and is therefore indirectly dependent on the pump power [25]. The effective Raman gain can be determined from the model of an intracavity Raman laser, such as those reported in [13] and [25]. To calculate the effective Raman gain we need to know the total round trip loss for the Raman laser, the fundamental intracavity power and the beam sizes of both the fundamental and the Raman fields along the diamond. The total round trip loss for the Raman laser (L_R) is given by the summation of the HR mirrors transmission (T_{FM2} = T_{M3} ~0.001% at 740 nm), the dichroic mirror transmission (T_{DCM}~0.01% at 740 nm), the output coupler transmission (T_{OC} = 1.5%), and the losses associated with the Raman medium. Here we assume $L_{diamond}$ = 1.4 ± 0.4% as we measured in Section 3, although we expect the absorption loss at 742 nm to be slightly lower than at 675 nm as the absorption coefficient of diamond is usually smaller at longer wavelengths [15, 17]. The total loss is given by:

$$L_R = L_{diamond} + 2T_{DCM} + 2T_{FM2} + T_{M3} + T_{OC} = 2.9 \pm 0.4\% \tag{1}$$

The effective Raman gain at the Raman threshold ($g_{eff,th}$) can be determined from the following equation [9]:

$$(1-L_R)\exp\left(4g_{eff,th}I_{f,th}l_{cr}\right) = (1-L_R)\exp\left(4g_{eff,th}P_{f,th}l_{cr}/A_{f,th}\right) = 1 \tag{2}$$

where L_R = 2.9 ± 0.4% is the total loss for the Raman laser, l_{cr} = 8 mm is the length of the Raman medium, $P_{f,th}$ = 10 W is the fundamental intracavity power at the Raman threshold, and $A_{f,th} = \pi\omega_{f,th}^2$ is the average pumped area along the Raman medium at the Raman threshold. Note that, compared with [9], the backward stimulated Raman scattering is taken into account with an additional factor of 2 in the exponential. For the calculation of the average beam size (ω) we use the definition given in [13]:

$$\omega = \sqrt{\omega_0^2 + \frac{M^4\lambda^2 l_{cr}^{\ 2}}{12\pi^2\omega_0^2 n^2}} \tag{3}$$

where ω_0 is the TEM_{00} beam waist radius, M^2 the beam quality factor, λ the laser vacuum wavelength, and n the refractive index of the Raman medium. The TEM_{00} beam waist radius of the SDL beam at the Raman medium was calculated to be 19.5 μm. We did not measure the beam quality (M^2) of the SDL at the Raman threshold, but it is reasonable to assume it was less than 1.8 (as measured at the ~65 mW output power), thus the average pumped area ($A_{f,th}$) and the effective Raman gain at the Raman threshold ($g_{eff,th}$) are estimated to be < $2.34 \cdot 10^3$ μm^2 and < 21.5 ± 3.0 cm/GW, respectively.

At pump powers greater than the Raman threshold the effective Raman gain (g_{eff}) can be calculated from the model of the intracavity Raman laser [25]:

$$g_{eff} = \frac{L_R A_e}{4 l_{cr} P_f} \tag{4}$$

where $A_e = (\int I_f I_R \, dA)^{-1}$ is the effective area where Raman conversion occurs, and I_f and I_R are the normalized intensity profiles of the fundamental and the Raman fields, respectively. With Gaussian transverse profiles the definition of the effective area becomes $A_e = (\pi/2) \cdot (\omega_f^2 + \omega_R^2)$, where ω_f and ω_R are the beam spot radius of the fundamental and the Raman fields, respectively [25]. At ~65 mW output power the fundamental intracavity power (P_f) was measured to be 12 W, while the beam quality factors of the SDL and the Raman laser were 1.8 and 1.55, respectively, hence the effective area (A_e) was $2.28 \cdot 10^3$ μm^2. Thus the effective Raman gain (g_{eff}) at ~65 mW output power is estimated to be 17.2 ± 2.4 cm/GW.

Comprehensive literature analyses of the available data on the Raman gain coefficient in diamond have been carried out in [17] and [26]. Here it is worth noting that the reported values cover a broad range due to uncertainties in the diamond orientation, pump polarization with respect to the diamond crystallographic axes, pump emission linewidth, sample quality, and differences in the methodology for the evaluation of the Raman gain coefficient [17, 26-28]. On the other hand, it is well known that the Raman gain coefficient is wavelength dependent, with increasingly larger values at shorter wavelengths [17, 26]. In the red spectral range the Raman gain coefficient of diamond has previously been measured to be ~6.9 cm/GW at 694 nm for pump propagation along <111> [27] and 41±4 cm/GW at 670 nm for pump propagation along <110> and pump polarization parallel to <111> [17]. Measurements of polarizability and Raman scattering efficiency at different wavelengths (including red), from which it is possible to estimate the Raman gain coefficient as shown in [26], are reported in [28], but the pump source was unpolarized. Therefore only the measurement reported in [17] can be directly compared to the system reported here; however, this value is at the top end of the range in the literature and somewhat larger than the effective Raman gain calculated above. A reduced effective Raman gain may be due to a suboptimal spatial overlap between the fundamental and the Stokes fields, and to the relatively broad spectral emission of the SDL, whose emission linewidth (~1 cm^{-1}) was comparable to the spontaneous Raman linewidth of diamond (1 - 2.5 cm^{-1} [14, 29]).

With narrower SDL emission linewidth the performance of this system could be improved in terms of Raman threshold and overall efficiency. One recent work has shown that the effective Raman gain of an intracavity Raman laser can be enhanced by inserting intracavity etalons [30], albeit with the detrimental effect of increasing the cavity losses. Limiting the total cavity losses is crucial for the overall efficiency, and SDLs, as low gain lasers, are particularly susceptible to loss. A more promising route to improved efficiency is therefore with the expected further advances in the growth of ultra-low loss, low birefringent CVD diamonds which will be beneficial for the reduction of absorption losses within both the heatspreader and the Raman medium. Indeed, we note that the absorption loss measured for the diamond used in this work is not state-of-the-art.

6. Conclusion

We report, for the first time to our knowledge, a diamond Raman laser pumped by a visible semiconductor disk laser (SDL). We observed tunable emission from 736.6-750.4 nm, maximum output power of 82 mW at 744 nm, good beam quality (M^2~1.55) and narrow linewidth emission (≤0.05 nm). This work shows a novel way for semiconductor disk lasers to reach the 'therapeutic window' (700-800 nm). The output power achieved by this diamond Raman laser is higher than that obtained with a SDL based on InP QDs [7], and no sign of thermal rollover was observed. While the output power is clearly lower than that achieved by the frequency-doubled wafer fused SDL at higher wavelengths (1 W at 785 nm [8]), the optical conversion efficiencies of the two lasers are actually comparable (~2%). This system is therefore promising for future power scaling, and is indeed currently limited by the pump power. Moreover, unlike frequency-doubling, this laser can be spectrally tuned with no phase-matching requirements.

Acknowledgments

The authors would like to thank Dr Andrey Krysa of the EPSRC National Centre for III-V Technologies for growing the SDL gain structure, and Dr Ian Friel of Element Six Ltd for providing the diamond sample. This work was supported by the Engineering and Physical Sciences Research Council (ESPRC), UK, under grant EP/I022791/1, the European Research Council under grant 278389, and by Fraunhofer UK Ltd and the Royal Academy of Engineering via a research chair.